A Unique strategy for probing *in-situ* NO for screening the neuroinflammatory phenotypes against SARS-CoV-2 RNA in phagocytotic microglia

Subrata Munan,[a] Abir Mondal,[b] Shailja Singh,*[c] Soumya Pati,*[b] and Animesh Samanta*[a]

[a] Molecular Sensors and Therapeutics (MST) Research Laboratory, Department of Chemistry, School of Natural Sciences, Shiv Nadar Institution of Eminence (SNIoE), Delhi NCR, NH 91, Tehsil Dadri, Greater Noida, Uttar Pradesh, India 201314

*[a] Email: animesh.samanta@snu.edu.in

[b] Department of Life Sciences, School of Natural Sciences, Shiv Nadar Institution of Eminence (SNIoE), Delhi NCR, NH 91, Tehsil Dadri, Greater Noida, Uttar Pradesh, India 201314

*[b] E-mail: soumya.pati@snu.edu.in

[c] Special Centre for Molecular Medicine, Jawaharlal Nehru University, New Delhi 110067, India

*[b] E-mail: shailjasingh@mail.jnu.ac.in

KEYWORDS: Fluorescent Probe; Lysosome; Nitric Oxide; Microglia; Phagocytosis; SARS-CoV2 RNA.

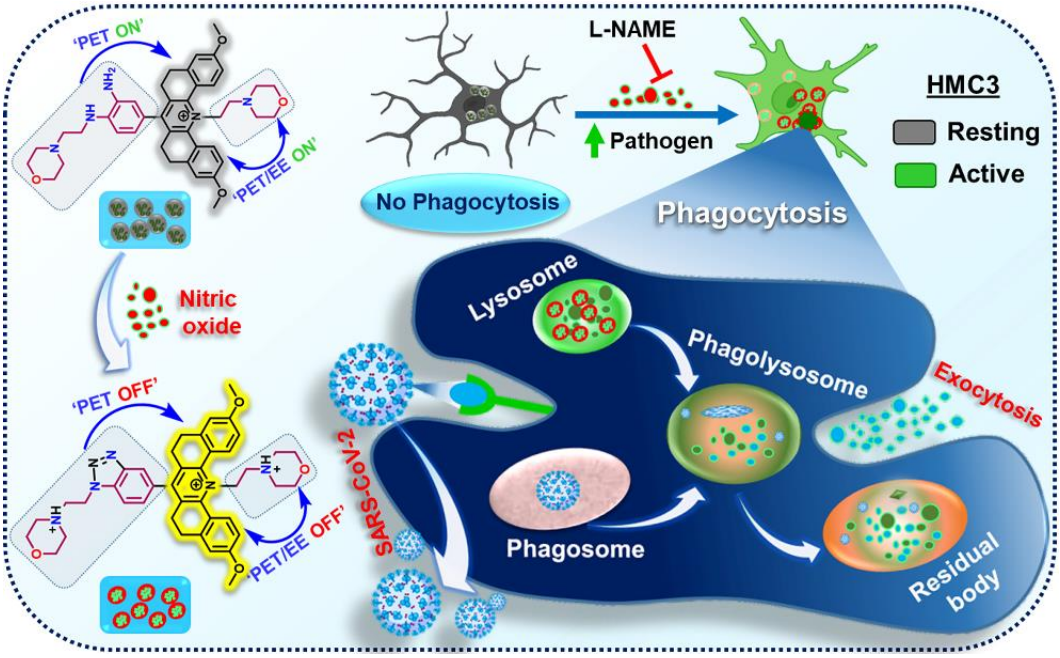

Abstract. The severe acute respiratory (SARS-CoV-2) jeopardized public health by causing significant morbidity and mortality among people with pre-existing physiological dysfunction caused by aging, diabetes, hypertension, and obesity. Besides, patients with severe infections are more likely to have neuro-inflammation and higher mortality risk. Neuroinflammation is majorly caused by activating the brain's residential macrophage cells called microglia, which increases the generation of reactive species including nitric oxide via the iNOS pathway. In addition, NO regulates lysosomal functions and exhibits complex effects on lysosomal machinery to neutralize foreign pathogens through phagocytosis and improves host-defense inflammatory response. To date, lack of efficient probes to monitor lysosomal NO and phagocytosis processes in least explored human microglia during SARS-CoV-2 infection. Herein, a unique design strategy was adopted for the first time by avoiding the conventional control amination reaction approach to develop lysosomal specific-NO probe, **PDM-NO**, which can discriminate activated microglia from its resting state. The nonfluorescent probe at physiological pH exhibits turn-on response towards NO only at

https://doi.org/10.26434/chemrxiv-2023-vk4f4 **ORCID:** https://orcid.org/0000-0002-6484-9017 Content not peer-reviewed by ChemRxiv. **License:** CC BY-NC-ND 4.0

lysosomal pH (4.5-5.5). **PDM-NO** demonstrated lysosomal specificity in activated HMC3 cells and enabled monitoring phagocytosis process with a several advantages compared to commercial *E.* coli bio-particles. Moreover, this probe can effectively map the overexpression and dynamics of lysosomal NO levels against SARS-CoV-2 RNA virus-induced neuroinflammation in HMC3. Thus, lysosome-specific **PDM-NO** is a potential fluorescent marker for detecting RNA virus infection in human microglia and excellent molecular probe for monitoring phagocytosis during neuroinflammation. It could be a useful commercial probe in future for screening viral activity and neuroinflammation for diagnosis of neurological diseases.

Introduction. The microglia, macrophage cells located in the central nervous system (CNS), plays a pivotal role in various neurological processes, such as neurogenesis, myelination, synaptic pruning, and inflammation.[1–3] The activated microglia migrate to the site of injury or pathogen invasion to respond and start secreting pro/anti-inflammatory cytokines and neurotoxic molecules, such as interleukin (IL)-6, IL-1β, tumour necrosis factor (TNF)-α, and nitric oxide (NO) respectively, leading to neuronal dysfunction.[4–8] The activation also enables microglia to engulf foreign pathogens through phagocytosis, where phagosomes containing the pathogens fuse with acidic lysosomes to remove damaged neurons, debris, and apoptotic cells.[9–12] During activation, microglia upregulate inducible nitric oxide synthase (iNOS), releasing excess nitric oxide (NO) that influences autophagy through interactions with the lysosomal machinery.[13–17] Prolonged activation of microglia can lead to neuronal loss and contribute to neuroinflammatory and neurodegenerative diseases.[4,17–21] While rodent models have been extensively used to study microglial cell activation and functions, research on human microglia has been limited due to the lack of availability of HMC3 cells.[22]

Recent reports have shown that patients suffering from Long-COVID syndrome (LCS) and post-COVID-19 syndrome (PCS) exhibit neurological alterations, indicating that SARS-CoV-2 impact on cellular dysfunction, and lysosomal egress pathways.[23–28] Notably, oxidative stress appears to be a major driver of the pathophysiological mechanisms underlying LCS leading to the propagation of neuro-inflammation.[29–32] In severe COVID-19 infections, patients are more likely to experience microgliosis, immune cell accumulation, and a higher risk of mortality.[33,34] Recent studies have revealed that single-stranded RNA fragments from the SARS-CoV-2 genome can activate innate immune receptors, triggering the secretion of pro-inflammatory cytokines.[35,36] However, understanding the dynamics of nitric oxide (NO) in neuroinflammation related to COVID-19 linked neurological symptoms in the human brain is currently limited due to the lack of efficient cellular models for studying these processes.

Therefore, the development of a probe that can rapidly, sensitively, and selectively sense in-situ lysosomal NO in HMC3 cells and study phagocytosis during infections would provide a unique platform for diagnosing and understanding inflammatory diseases. In recent times, small molecular fluorescent probes have gained prominence as an alternative to ELISA for quantifying NO due to their simplicity, high sensitivity, and non-invasive real-time imaging capability.[37–41] Although several NO-specific fluorescent probes have been developed, very few can detect lysosomal NO, and none of them have been reported to study neuroinflammation in HMC3. The use of o-diaminophenyl (OPD) ligands with different fluorophores has been common in developing NO-specific fluorescent probes, following pioneering research by the Nagano group.[42] Secondary amine (N-methyl aniline) conjugated fluorophores have also been found to be efficient NO probes due to their faster reaction with NO.[43] The Nagano group further reported the use of

https://doi.org/10.26434/chemrxiv-2023-vk4f4 **ORCID:** https://orcid.org/0000-0002-6484-9017 Content not peer-reviewed by ChemRxiv. **License:** CC BY-NC-ND 4.0

three different cores, including rhodamine,[44] fluorescein,[45] and BODIPY,[46] with controlled methylation of OPD derivatives. However, the tedious control amination process results in N-methyl 3,4-diamino benzene/N1-methylbenzene-1,2-diamine conjugated fluorophores (Scheme 1). While a few more probes have been developed, most of them suffer from inefficient synthesis, reactivity to NO, and small Stokes shifts associated with autofluorescence. Additionally, *in vitro* studies, including cellular experiments, often involve the use of high percentages of toxic organic solvents as co-solvents (Table S2).

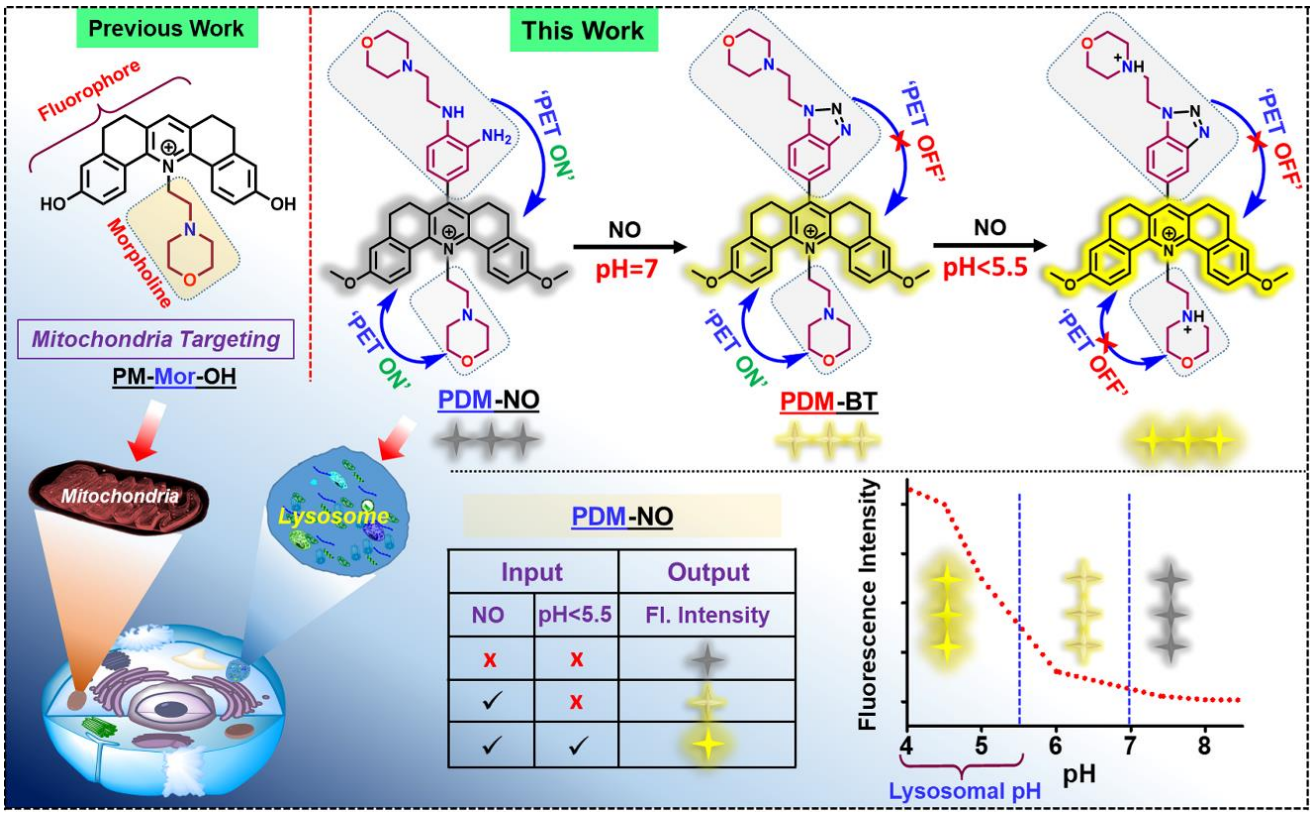

Figure 1. Design principle and proposed mechanism of **PDM-NO** for mapping nitric oxide in acidic cellular organelles (Lysosome).

Herein, we developed a unique synthesis strategy to render secondary amine of OPD that overcome control methylation and double morpholine tagged fluorescent probe, **PDM-NO** for targeting lysosomes exclusively (Figure 1). It demonstrates a turn-on florescence response to NO within lysosomal pH window. The morpholine amine tagged-OPD serves as an effective NO trapper, while a novel pentacyclic pyridinium fluorophore acts as a signal transducer. The inclusion of morpholine units enables specific targeting of lysosomes. The pH-dependent emission for NO sensing is thoroughly explained by employing photoinduced electron transfer (PET) through TD-DFT/PCM calculations. The real-time Q-PCR confirms pro-inflammatory gene expression in activated HMC3 cells. Additionally, the analysis of confocal fluorescence images successfully detects exogenous NO in lysosomes in activated HMC3 for the first time. Moreover, the probe efficiently monitors in-situ iNOS-induced NO in lysosomes and accurately observes the phagocytosis process. The probe also demonstrates the capability to detect SARS-CoV-2 infection in activated HMC3 cells through lysosomal NO imaging. Finally, phagocytosis was monitored by the probe during SARS-CoV-2 infection. Thus, **PDM-NO** is a promising fluorescent probe for unveiling a new horizon in neuronal cells, particularly during neuroinflammation.

https://doi.org/10.26434/chemrxiv-2023-vk4f4 **ORCID:** https://orcid.org/0000-0002-6484-9017 Content not peer-reviewed by ChemRxiv. **License:** CC BY-NC-ND 4.0

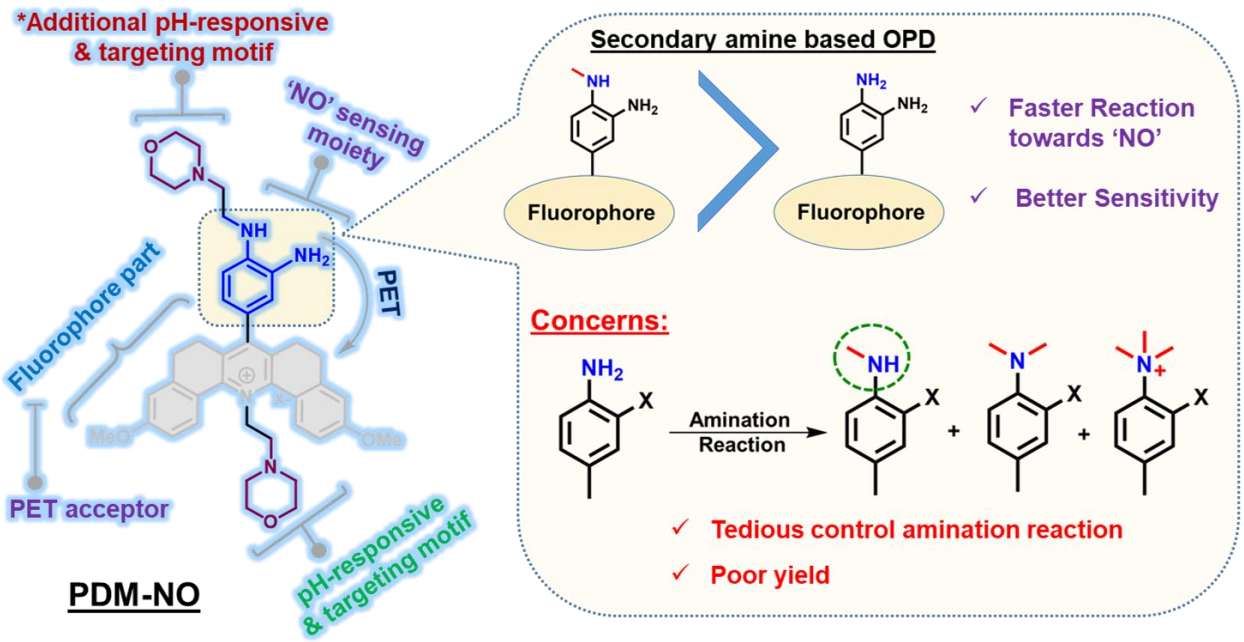

Scheme 1. *Schematic representation of newly designed fluorescent probe,* ***PDM-NO*** *with its advantages on sensitivity, control reactivity compared to conventional OPD-based approach for NO sensing.*

RESULTS AND DISCUSSION

Design and Synthetic demonstration of the probe. Recent studies have explored different strategies to enhance target specificity for specific organelles, including lysosomes, allowing for the regular monitoring of organelle functions. This provides invaluable information for investigating pathways associated with disease progression. One such strategy involves the use of weakly basic compounds that can accumulate in lysosomes due to their acidic vesicular structure,[47] while cationic amphipathic compounds are targeted to mitochondria.[48] In a recent report, we introduced a small molecular fluorescent probe, **PM-Mor-OH**, which is conjugated with a weakly basic morpholine amine (Figure 1).[49] Surprisingly, despite its weakly basic nature, the fluorophore demonstrated a preference for targeting mitochondria rather than lysosomes, likely due to its cationic properties. Here, we adopted two morpholine ligands to introduce more basic nature into cationic pyridinium fluorophore to develop **PDM-NO** for targeting lysosomes. It detects exclusively NO within lysosomal pH window (4.5-5.7) (Figure 1). The secondary amine, N-methyl 3,4-diamino benzene (NM-OPD), demonstrates higher reactivity towards NO compared to its primary amine counterpart (3,4-diamino benzene known as OPD), resulting in improved sensitivity and higher enhancement (Scheme 1 and Figure 2).

https://doi.org/10.26434/chemrxiv-2023-vk4f4 **ORCID:** https://orcid.org/0000-0002-6484-9017 Content not peer-reviewed by ChemRxiv. **License:** CC BY-NC-ND 4.0

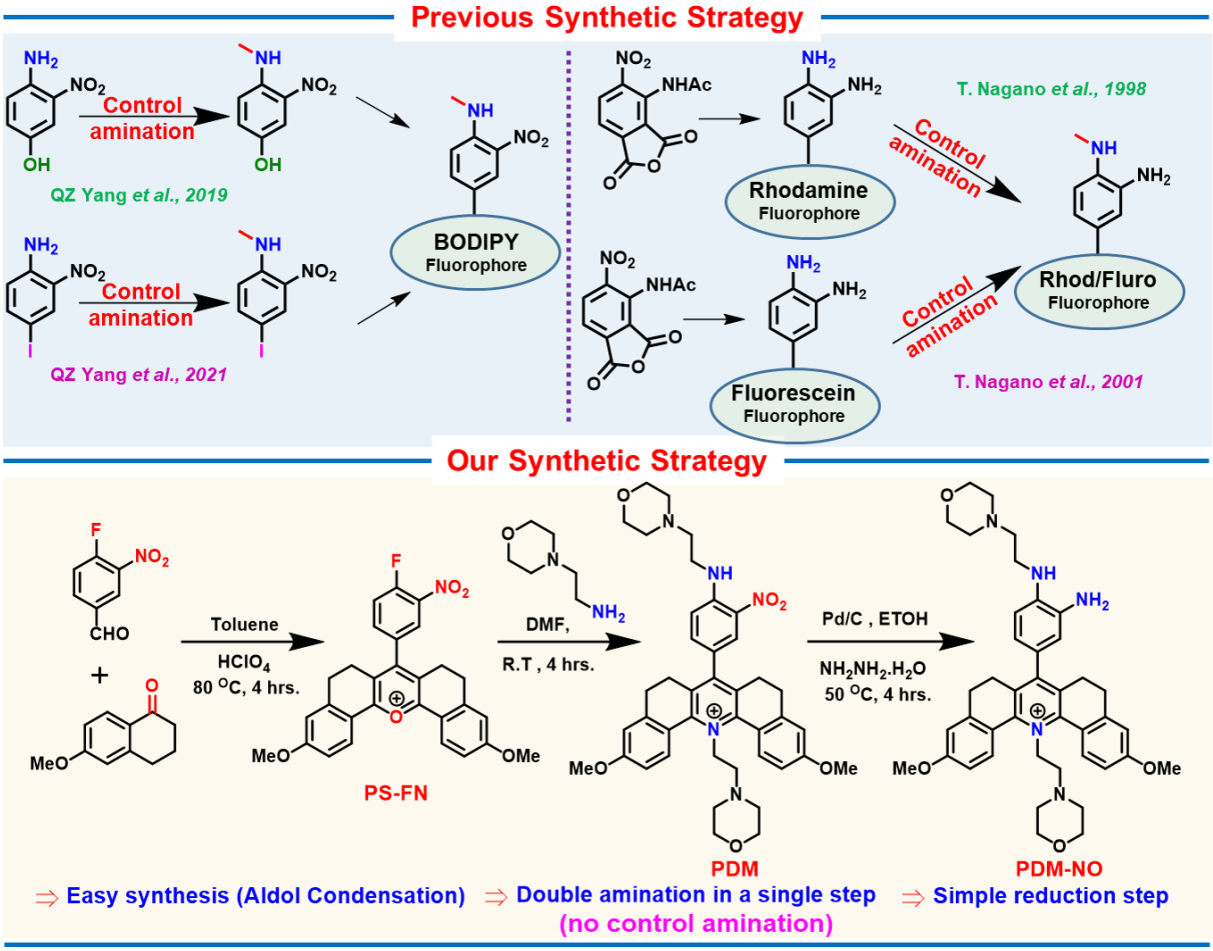

Scheme 2. *Synthetic Strategy difference among previously reported work and newly designed work. Synthesis of* ***PDM-NO****.*

Herein, we propose a simple design strategy to efficiently synthesize a secondary amine, N^1-(2-morpholinoethyl)-benzene-1,2-diamine tagged fluorophore, named as **PDM-NO** (Pyridinium-Di-Morpholine-Nitric Oxide), in an easy step from **PS-FN** (as shown in Scheme 2 and Scheme S3). To synthesize **PS-FN**, 1 equivalent of 4-fluoro-3-nitro-benzaldehyde was mixed with 2 equivalents of 6-methoxy-tetralone in the presence of a catalytic amount of perchloric acid, and the reaction was carried out at 80°C for 2 hours, yielding 67%. Subsequently, **PS-FN** was treated with 2.5 equivalents of 2-morpholinoethan-1-amine to obtain **PDM** which was further reduced using hydrazine and Pd (C) to obtain the final probe. The product was purified by column chromatography with 65% yield. The intermediates and the final probe were characterized by ^{1}H-NMR, ^{13}C-NMR, and HRMS (Scheme 2 & S1−S4). In summary, a unique design and straightforward synthesis of secondary aromatic amine, a derivative of OPD is adopted that reacts with NO to show efficient turn on fluorescence response in acidic window.

Spectroscopic Study. Organelle-specific fluorescent probe are always invaluable tools for the investigation of disease-relevant pathways if the probe exhibits good optical properties and low cytotoxicity. Hence, we first elucidated spectroscopic properties of **PDM-NO,** including absorbance maxima (λ_{max}), emission maxima (λ_{max}), Stokes shift, relative quantum yield (Φ_F), and molar extinction coefficient ($\mathcal{E}$) in

https://doi.org/10.26434/chemrxiv-2023-vk4f4 **ORCID:** https://orcid.org/0000-0002-6484-9017 Content not peer-reviewed by ChemRxiv. **License:** CC BY-NC-ND 4.0

PBS buffer. The solubility of **PDM-NO** in water (DMSO: H_2O; 0.1/1000 μL) was evaluated, and it exhibited excellent solubility in an aqueous medium (Figure S1), allowing its use without the need for unsafe organic solvents typically used with other NO probes (Table S2). This attribute is advantageous for cellular imaging and avoids potential cytotoxicity associated with organic solvents used in other probes (Table S2). The **PDM-NO** showed an absorption and emission maxima at 420 nm and 585 nm respectively with large Stokes shift of 165 nm (6715.5 cm^{-1}) compared to the reported probes (Figure S2). The probe's large Stokes shift is beneficial for cellular imaging by setting a secondary filter that reduces the autofluorescence, resulting in improved image quality.

The probe exhibited minimal fluorescence (Φ_F=0.005) upon excitation at 420 nm, indicating low autofluorescence. Upon reaction with NO (DEA·NONOate: a commercially available NO donor with a half-life time of 16 min) at lysosomal pH 4.5, a remarkable fluorescence enhancement was observed, with a high Φ_F of 0.26. The probe demonstrated a fluorescence intensity enhancement of approximately 45.1 and 40.5-fold at pH 4.5 and 5.0, respectively, upon titration with 100 μM NO (1 µM probe) as shown in Figure 2e & S3. The probe's emission response to NO at pH 4.5-5 was rapid (Figure 2a and b), occurring in less than 7 minutes (Figure 2c and d). At physiological pH 7.4, the probe remained almost silent even after adding an excess of NO, indicating its suitability for lysosomal pH-specific imaging. The limit of detection for NO was determined to be 23.59 nM using the 3σ/k method with a high R^2=0.9973 (Figure 2f & Table S1), demonstrating its sensitivity in detecting low concentrations of NO. **PDM-NO** exhibited good photo-stability in PBS buffer at pH 4.5 during continuous irradiation of 450W mercury lamp for 30 min in the presence of 100 μM NO (Figure S4), ensuring reliable and consistent fluorescence measurements during imaging experiments.

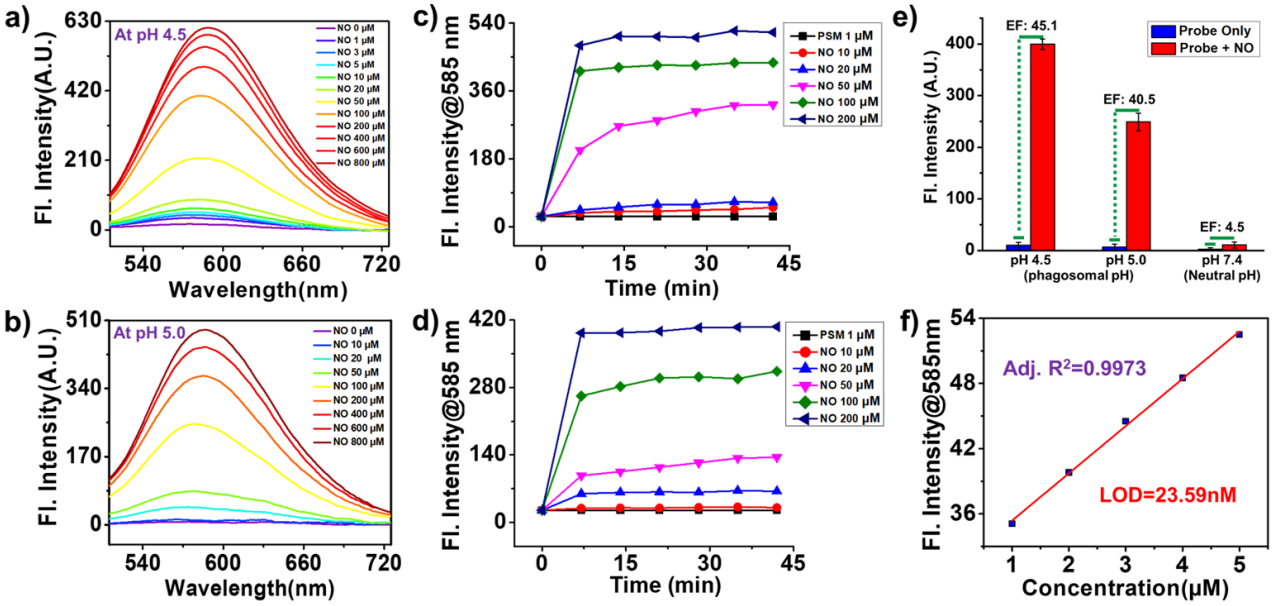

Figure 2. *Fluorescence spectra of* ***PDM-NO*** *(1 µM) Probe treated with DEA·NONOate (0−800 µM) in PBS buffer (10 mM) at* ***a)*** *pH 4.5 and* ***b)*** *5.0 respectively (λ_{ex}. 420 nm). Time-dependent fluorescence intensity changes of probe* ***PDM-NO*** *towards DEA·NONOate (10-200 µM). Each spectrum was recorded in PBS buffer (10 mM) at* ***c)*** *pH 4.5 and* ***d)*** *5.0 respectively (λ_{ex}. 420 nm, λ_{em}. 585 nm).* ***e)*** *Titration of*

https://doi.org/10.26434/chemrxiv-2023-vk4f4 **ORCID:** https://orcid.org/0000-0002-6484-9017 Content not peer-reviewed by ChemRxiv. **License:** CC BY-NC-ND 4.0

100 μM DEA· NONOate with the probe 1 μM shows a fluorescence intensity enhancement with approximately 45.1 and 40.5-fold at pH 4.5 and 5.0, respectively. 'EF' stands for fold of enhancement. ***f)*** *Limit of detection (LOD) of the probe was determined to be 23.59 nM using 3σ/k method with R^2=0.9973.*

The reaction of **PDM-NO** with NO led to the formation of a benzotriazole derivative, **PDM-BT**, as confirmed by HRMS analysis (Figure 1 and S5). The electron transfer from the OPD derivative was inhibited upon the formation of benzotriazole derivative, resulting in turn-on fluorescence at physiological pH (pH 7.4). However, the fluorescence intensity was enhanced only 4.5-fold (Figure 2e). At lysosomal pH (pH 4.0 to 5.7), after protonation of the morpholine units, the fluorescence intensity was drastically enhanced (Figure 2e). The underlying principles of these turn-on optical properties were explained using TD-DFT/PCM theoretical calculations.

Mechanistic investigation using TD-DFT. Next, we studied using theoretical calculation to understand the modulation of optical properties of the probe alone and after the reaction with NO at variable pH. The optimized geometry of the probe, **PDM-NO** and the products **PDM-BT** at the electronic ground state was first optimized using density functional theorem (DFT) at the B3LYP level of theory and 6-311++G (d, p) basic set through the polarizable continuum model (PCM), using water as a solvent. The time-dependent density functional theorem (TD-DFT) was employed for the vertical excitation (absorption) by the corrected linear response (cLR) method using the non-equilibrium solvation (PISALR) model. The S1 state of **PDM-NO** showed a clear excited charge transfer (CT) state. The transition occurred from the highest occupied molecular orbital (HOMO) to the lowest unoccupied molecular orbital (LUMO). HOMO was predominantly located on the donor part (**OPD-Mor**) and LUMO was on the fluorophore part (**PSM**) (Figure 3a). The overlapping area between the HOMO and LUMO was low, corresponding to its lower oscillator strength (*f*=0.15), suggesting the weak-fluorescent property (Table S3). To explain the quenching phenomenon, the role of **OPD-Mor** and Morpholine (**Mor**) moiety were considered as both were attached to the acceptor part of the fluorophore, denoted as **PSM**. Firstly, as shown in Figure 3b, the HOMO of **OPD-Mor** moiety is present above the HOMO of **PSM**, suggesting photo-induced electron transfer (PET) is feasible to quench the fluorescence property. Next, the distribution of localized electron density of **PDM-BT** was also evaluated (Figure 3a). HOMO and LUMO were located on the **PSM** and a high overlapping area between the MOs led to high oscillator strength (*f*=0.57) in the S1 state (Table S3). Consequently, the de-excitation/emission of **PDM-BT** in the S1 state showed high oscillator strength 0.70 compared to unreacted **PDM-NO** (*f*<0.01). It also again confirms the turn-on emission property (Table S4) by suppressing the quenching pathway (PET).

Subsequently, the morpholine group attached fluorophore shows quenching in **PSM-Mor** (Figure S6). As shown in Figure 3c and d, the HOMO energy of the morpholine unit (**Mor)**, and **PSM** exhibited almost similar (-6.23 eV). Thus, the possibility of electron exchange (EE) or PET between the HOMOs of both **PSM** and **Mor**, may lead to quenching the fluorophore. In acidic lysosomal pH (pH 4.5~5.7), the HOMO energy of protonated morpholine (**MorH**$^+$) decreased to -8.07 eV from -6.23 (**Mor**) (Figure 3d). Hence, neither EE nor PET processes are feasible to quench the fluorescence properties.

https://doi.org/10.26434/chemrxiv-2023-vk4f4 **ORCID:** https://orcid.org/0000-0002-6484-9017 Content not peer-reviewed by ChemRxiv. **License:** CC BY-NC-ND 4.0

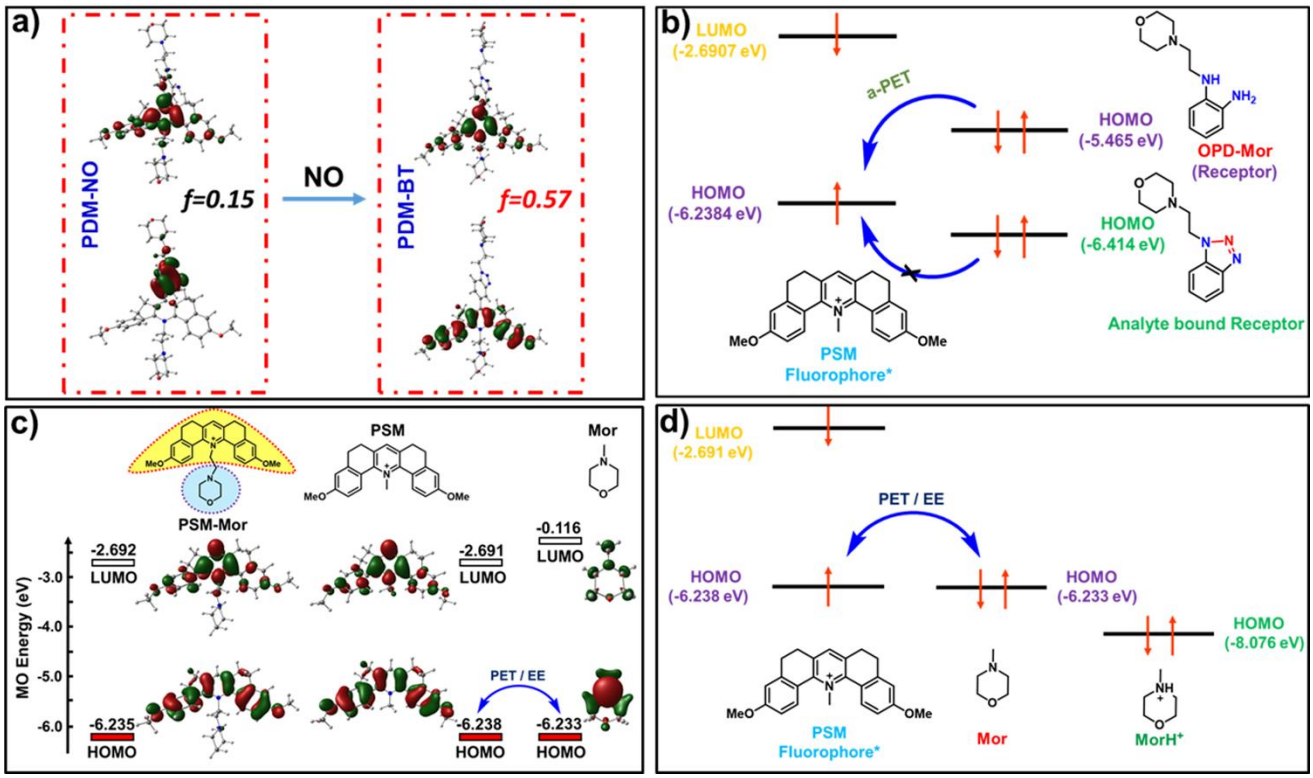

Figure 3. ***a)*** *Theoretical representation of* ***PDM-NO*** *and* ***PDM-BT*** *in the S1 state. The localized electronic charge distribution in HOMO and LUMO, and their corresponding variable oscillator strengths.* ***b)*** *Theoretical representation of Photoinduced electron transfer (a-PET) process from* ***OPD-Mor*** *moiety.* ***c)*** *Localized electronic charge distribution in HOMO and LUMO of* ***PSM-Mor***, ***PSM*** *and* ***Mor*** *moiety and prediction of electron exchange (EE) process.* ***d)*** *Theoretical representation of electron exchange (EE) process from* ***Mor*** *moiety and in acidic pH neither EE nor PET.*

Selectivity Test. The specificity towards NO of the probe is essential for the selective detection of NO in a complex cellular environment. Thus, we recorded the emission intensity at 585 nm of **PDM-NO** with NO (100 μM) and several biologically relevant analysts, including metal ions [Na^+, K^+, Co^{2+}, Zn^{2+}, Ni^{2+}, Ca^{2+}, Mg^{2+}, Cu^{2+}, Fe^{2+}, Fe^{3+}, NH4$^+$; 500 μM], anions [F^-, Cl^-, CO_3^{2-}, HCO_3^- , Cr2O_7^-, tBuO$^-$; 500 μM], Sucrose, amino acids [Gly, Ala; 500 μM], bio thiols [Cys, GSH; 500 μM], reactive oxygen species [OH^-, KO_2, HOCl, H_2O_2, NO_2^-, NO; 100 μM], and reactive carbonyl species [FA, MGO, GO; 100 μM] at PBS buffer (10 mM, pH 7.4). As shown in Figure 4, none of the analysts shows significant fluorescence intensity change with the probe **PDM-NO**, except for a small fluorescence change for the trivalent metal ions. The probe only responded with NO, suggesting **PDM-NO** is a potential probe for further investigating the imbalance of NO in the lysosomes.

https://doi.org/10.26434/chemrxiv-2023-vk4f4 **ORCID:** https://orcid.org/0000-0002-6484-9017 Content not peer-reviewed by ChemRxiv. **License:** CC BY-NC-ND 4.0

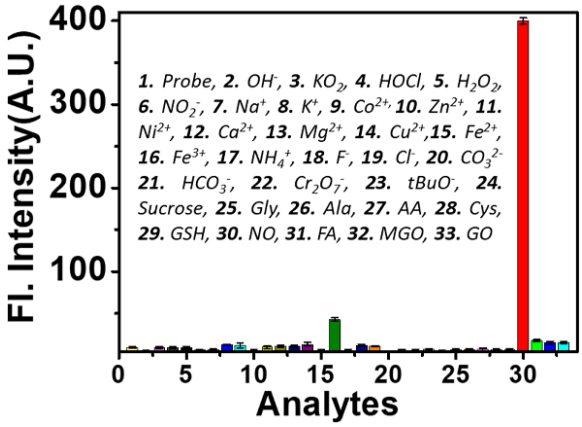

Figure 4. *1 μM* ***PDM-NO*** *was taken in PBS buffer at pH 4.5 in room temperature and emission was measured (λ_{ex}. 420 nm, λ_{em}. 585 nm). Then different biological analytes are added in that solution and emission was taken at the same excitation wavelength.*

Cytotoxicity of PDM-NO in HMC3. The biocompatibility of the developed NO-specific fluorescent probe, **PDM-NO**, within the permissive concentration range, is extremely crucial for conducting further experiments. To assess this, we initially evaluated the cytotoxicity of the probe in the human microglia clone 3 (HMC3) cell line using the methyl thiazolyl tetrazolium (MTT) assay (Figure S7). The probe was tested at various concentrations ranging from 1 μM to 50 μM. Remarkably, at a concentration of 10 μM, the **PDM-NO** probe exhibited > 90% cell viability. This result indicates its good biocompatibility within this concentration range and consequently, we selected 10 μM as the appropriate concentration for the subsequent cellular imaging study.

q-PCR analysis for Activated HMC3. Microglia cells can be activated under diverse signaling cascades triggered by both intrinsic and extrinsic stimulus including pathogen-associated molecular pattern molecules (PAMPs) (Figure 5a). It is also known that Interleukin-1β (IL-1β) and TNF-α (tumor necrosis factor-alpha) plays a crucial role as a pro-inflammatory cytokine, upregulating and secreted as part of the primary host defense against various PAMPs.[50] To induce activation and promote M1 polarization (pro-inflammatory phenotype) of human microglia cells, we treated HMC3 cells with LPS (lipopolysaccharide) and IFN-γ (interferon-gamma) for overnight in culture. To confirm the activation of microglia cells, we performed real-time quantitative polymerase chain reaction (Q-PCR) and quantified the mRNA expression levels of IL-1β and TNF-α (Figure 5b). Our data revealed a significant 10-15-fold increase in the expression of TNF-α in microglia cells activated with either LPS or a combination of LPS and IFN-γ, compared to the control group. Besides, we also observed 2-fold increase in IL-1β in both conditions as compared to the control. These results indicated successful activation of the microglia cells and the induction of a pro-inflammatory response under the given conditions.

https://doi.org/10.26434/chemrxiv-2023-vk4f4 **ORCID:** https://orcid.org/0000-0002-6484-9017 Content not peer-reviewed by ChemRxiv. **License:** CC BY-NC-ND 4.0

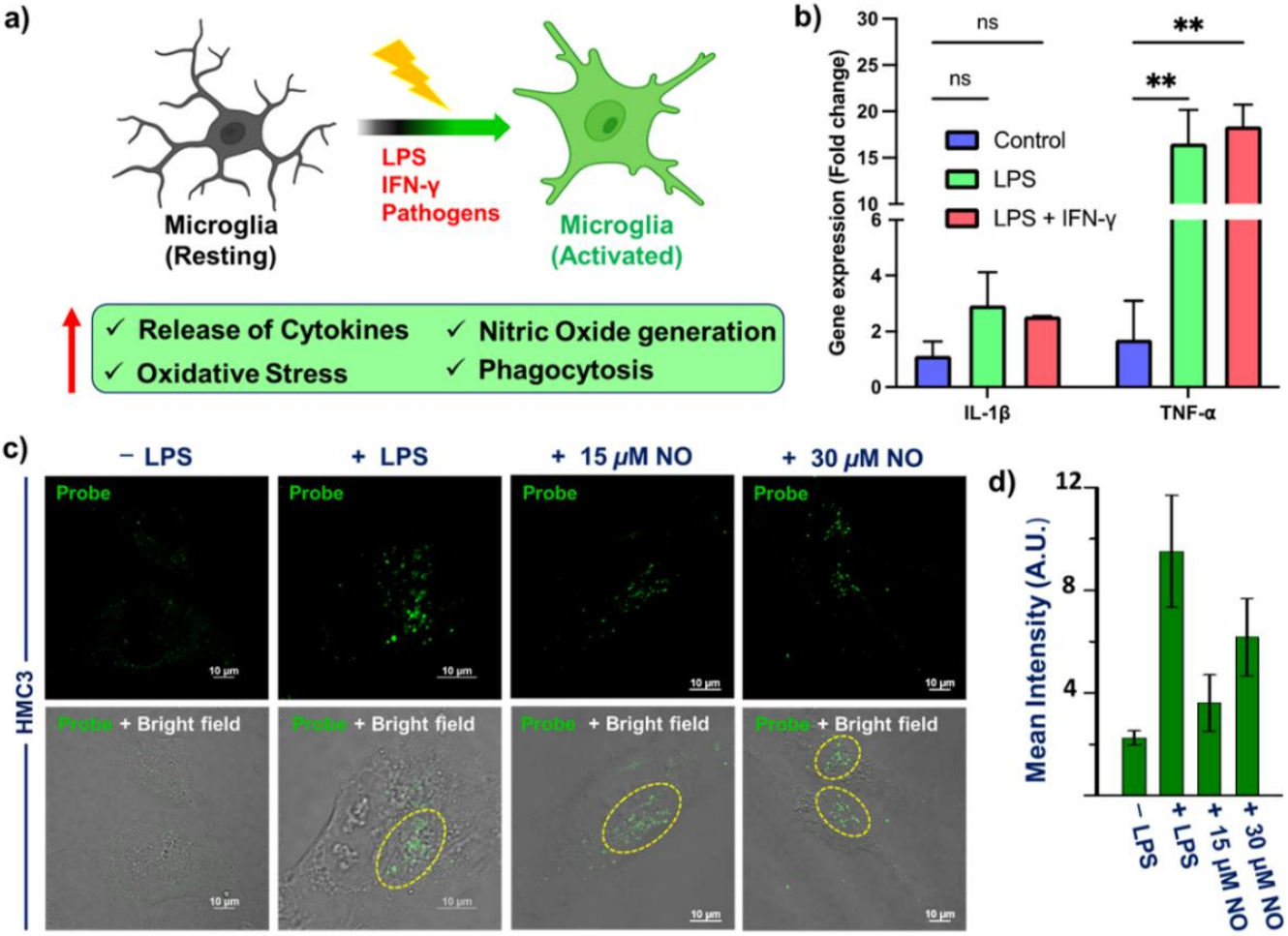

Figure 5. ***a)*** *Schematic representation of HMC3 cells activation by different types of intrinsic and extrinsic factors and their responses in activated HMC3.* ***b)*** *Q-PCR validation of pro-inflammatory markers (IL-1β and TNF-α) gene expression in response to different stimuli. Data represent the means ± SEM (n = 3). * shows significance values compared to control, * $p \leq 0.05$, ** $p \leq 0.01$. Statistical analysis was performed using Two-way ANOVA.* ***c)*** *The cells were incubated with* ***PDM-NO*** *for 15 min after the cells were stimulated without/with LPS (1 μg/ ml) at 37 °C for 24 hrs and with exogenous NO (15 and 30 μM) for 15 min. Images were acquired in a confocal microscope in the green channel, 550−600 nm, ex. 488 nm. The marked yellow circle represents the probe was stained brightly in a colony of distinct activated HMC3. The image scale bar is 10 μm. Images were captured using a 60X oil emersion lens with 2X zoom. d) Mean intensity image profile of figure 'c' without/with the stimulated condition.*

NO imaging in HMC3. As **PDM-NO** exhibits a turn-on fluorescence response towards NO, we further examined the sensing ability of NO in HMC3 cells. As the probe was non-fluorescent, the cellular imaging experiments were performed without washing, which minimizes the additional effort for mapping nitric oxide in cells. Reactive NO is synthesized from L-arginine by activating the iNOS enzyme, which was induced by treating bacterial lipopolysaccharide (LPS) and interferon-γ (IFNγ) in living HMC3 cells.[50,51] Cells treated only with the probe, **PDM-NO** (10 μM), showed a negligible green fluorescence, but LPS-treated cells along with the probe showed a bright green fluorescence (Figure 5c & d). This observation suggests that the probe is specific towards endogenous nitric oxide detection. Next, HMC3 cells were treated with variable amounts of NO (DEA·NONOate) at 37 °C in Opti-MEM media for 15 minutes

https://doi.org/10.26434/chemrxiv-2023-vk4f4 ORCID: https://orcid.org/0000-0002-6484-9017 Content not peer-reviewed by ChemRxiv. License: CC BY-NC-ND 4.0

before imaging (Figure 5c & d). The fluorescence intensity in cellular imaging from the colony of activated microglia (marked by the yellow circle) gradually increased with NO concentration in the treated cells. These results indicate that **PDM-NO** can detect exo/endogenous NO with an easy and fast response and may be localized in lysosomes.

Cellular Co-localization Experiment. The cellular co-localization experiments were performed in HMC3 cells after activating with LPS, and LPS/IFNγ for 24 h (Figure 6a). Confocal fluorescence image analysis after co-staining with the **PDM-NO** probe and LysoTracker Deep red for 15 minutes indicated maximum co-localization of the probe with lysosomes when co-activated with a mixture of LPS and IFNγ (Pearson's correlation coefficient 0.90) compared to LPS alone (Pearson's correlation coefficient 0.84) (Figure 6b). These results are well correlated with the previous report. Furthermore, to confirm the specificity of the **PDM-NO** to NO, we treated an inhibitor of nitric oxide synthase (iNOS) called L-NAME (L-N^G-Nitroarginine methyl ester) and a negligible fluorescence intensity was observed as expected (Figure 6b). Moreover, the line profile diagram shows the relative trend (LPS-IFNγ > LPS > LPS-IFNγ-L-NAME) of iNOS activity and its corresponding fluorescence intensity. Thus, our data clearly state that the **PDM-NO** is highly selective for NO and particularly co-localizes with lysosomes.

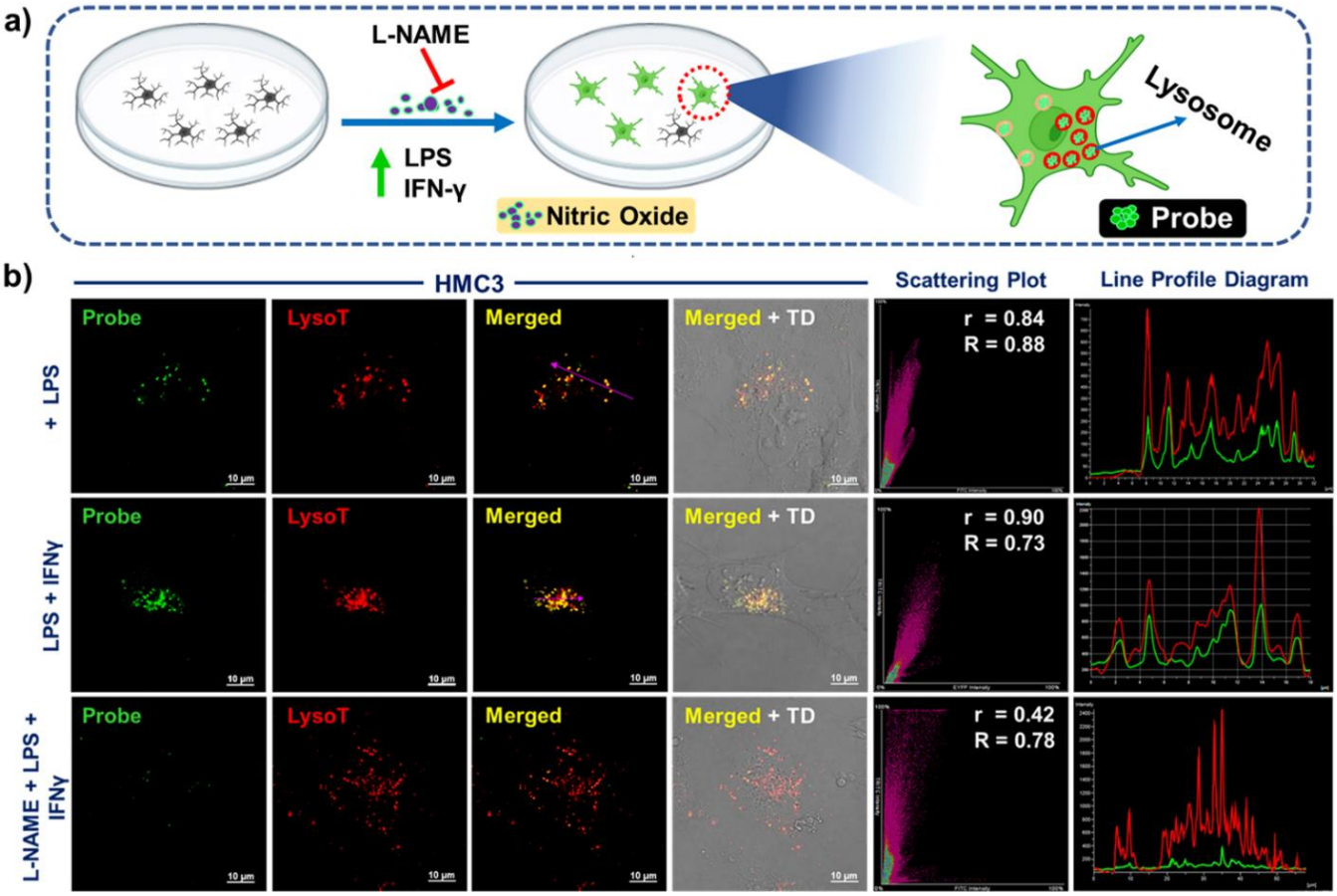

Figure 6. a) *Schematic demonstration of HMC3 cells activation and inhibition towards NO by different stimulators and activated state of HMC3 identification by using our* ***PDM-NO*** *probe.* ***b)*** *Confocal fluorescence images for intracellular localization study of* ***PDM-NO*** *probe. Here, the HMC3 cells were administrated with a probe that was previously treated with LPS; LPS/IFNγ; LPS/IFNγ/L-NAME. For labeling lysosomes, the cells were also treated with LysoTracker deep Red. Images were taken in the green*

https://doi.org/10.26434/chemrxiv-2023-vk4f4 **ORCID:** https://orcid.org/0000-0002-6484-9017 Content not peer-reviewed by ChemRxiv. **License:** CC BY-NC-ND 4.0

channel (550−600 nm, ex. 488 nm) for ***PDM-NO*** *and red channel (680−720 nm, ex. 640 nm) for LysoTracker deep Red and the corresponding scatter plots and line profile diagram were represented. The line profile diagrams of the merged images are shown by the arrow marks. In the scatter plot, "r" and "R" represent Pearson's correlation coefficient and Mander's overlap coefficient, respectively. The image scale bar is 10 μm. Images were captured using a 60X oil emersion lens with 2X zoom.*

Monitoring Phagocytosis. In response to pathogen invasion and injury, activated microglia undergo a highly ramified transformation and migrate to the lesion area through chemotaxis.[10,52] They release pro and anti-inflammatory cytokines along with nitric oxide (NO). High levels of NO serve as a cellular defense mechanism, expelling damaged cells and countering infections caused by invading pathogens.[20] Growing evidence suggests that lysosomes play a crucial role in removing pathogens through phagocytosis in the immune system.[53,54] Studies have reported that LPS/IFNγ activation leads to the release of NO by intracellular iNOS in microglia. This activation enables microglia to perform both immune functions and support neuronal health, depending on the NO levels.

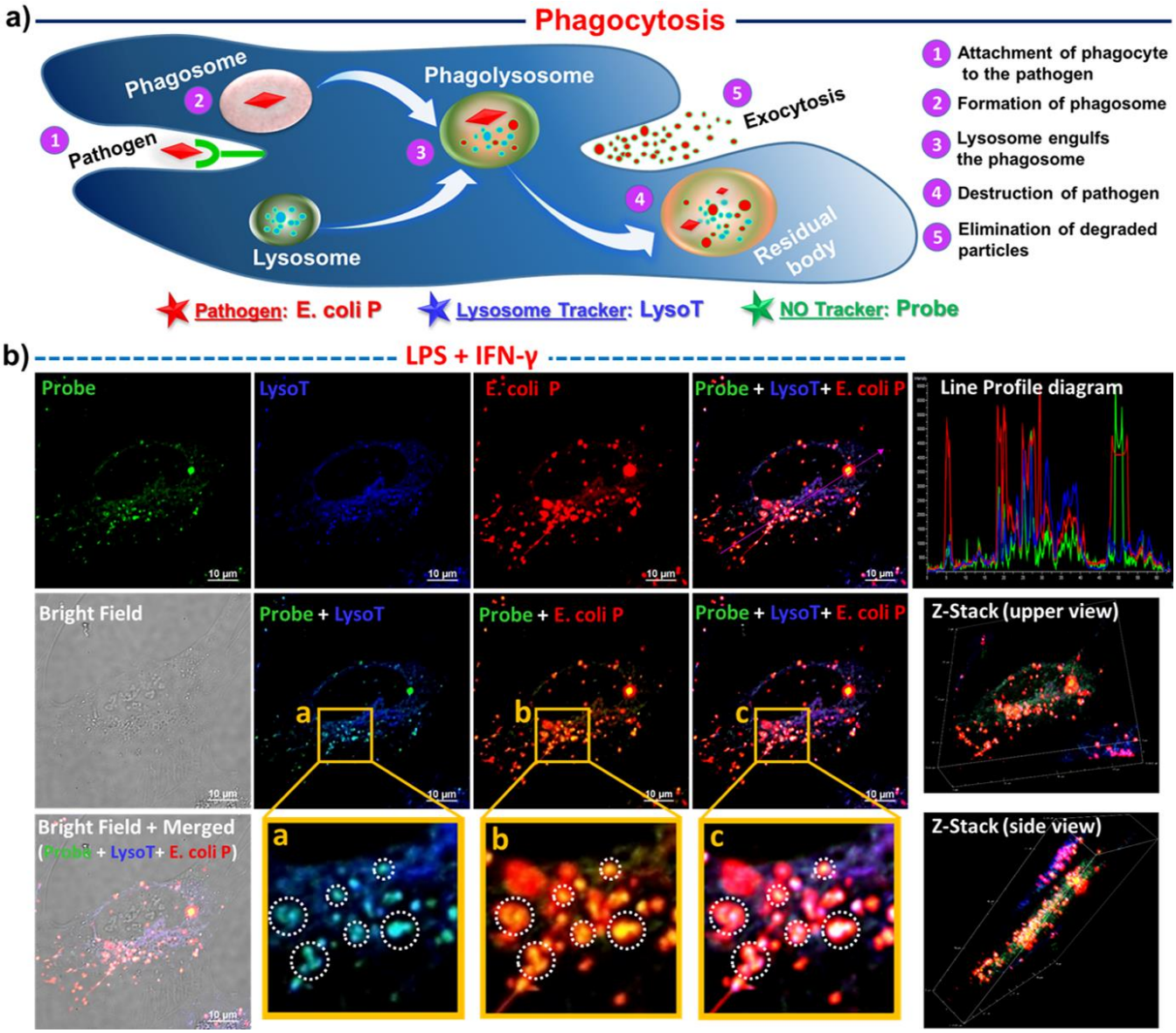

https://doi.org/10.26434/chemrxiv-2023-vk4f4 **ORCID:** https://orcid.org/0000-0002-6484-9017 Content not peer-reviewed by ChemRxiv. **License:** CC BY-NC-ND 4.0

Figure 7. a) *Schematic representation of the phagocytosis process against the pathogen in a cellular system.* ***b)*** *Confocal fluorescence images for NO-induced phagocytosis study by* ***PDM-NO*** *probe towards pHrodo-Red E. coli-bioparticles (E. coli. P). Here, the HMC3 cells were administrated with the probe, that was previously activated with LPS/IFNγ for 24 hrs. For labeling lysosomes, the cells were also treated with LysoTracker deep red. Images were taken in the green channel (550−600 nm, ex. 488 nm) for* ***PDM-NO****, pseudo blue channel for LysoTracker deep red (680−720 nm, ex. 640 nm), and red channel (620−650 nm, ex. 560 nm) for E. coli. P. The line profile diagrams of the merged images are shown by arrow marks. The image scale bar is 10 μm. Images were captured using a 60X oil emersion lens with 2X zoom. The zoom images marked a, b and c represent the perfect merged images of the probe with LysoTracker, the probe with E. coli. P, and the probe with LysoT+E. Coli. P respectively.*

Hence, understanding the role of lysosomal nitric oxide in activated microglia and its impact on microglial phagocytosis is crucial. To investigate the phagocytosis process, we treated pHrodo-Red E. coli-conjugated bioparticles (*E. coli. P*) as foreign pathogens and phagocytotic markers (Figure 7a). We used our lysosome-specific NO probe, **PDM-NO**, to monitor the phagocytosis process in both resting and activated microglia cells.

In Figure S8, we observed the cellular uptake of *E. coli. P* in LPS/IFNγ-treated cells (pre-treated for 24 hours) compared to non-treated HMC3 cells. Activated HMC3 cells exhibited the uptake of numerous *E. coli. P*, that could be detected at the single cell level, as shown in the z-stack images (Figure 7b and upper and side view). Moreover, activated HMC3 cells demonstrated good fluorescence signal overlap among **PDM-NO**, LysoTracker red, and E. coli. P (Figure 7b and S8), confirming the definite localization of *E. coli. P* to phagolysosomes. The internalization of bio-particles was trapped by the phagosomes and subsequently fused with lysosomes, as tracked by **PDM-NO**. In resting microglia, **PDM-NO** did not show phagosomes or the corresponding phagocytosis process (Figure S8). Overall, the results suggest that our lysosome-specific NO probe, **PDM-NO**, effectively monitors the phagocytosis process in activated microglia cells but not in resting microglia. The study highlights the importance of lysosomal nitric oxide in phagocytosis and provides valuable insights into the mechanisms of immune responses mediated by microglia.

Lysosomal NO detection against SARS-CoV-2 RNA in microglia. SARS-CoV-2 hijacks human host cells and replicating its own genome and generating progenies.[55] It utilizes the lysosomal egress pathway as one of the means to exit the host cell before invading various cell types and spreading throughout the body (Figure 8a).[56] Studies have shown that the spike protein of SARS-CoV-2 binds to the TLR2/TLR4 receptor on the surface of immune cells, leading to the activation of pro-inflammatory pathways, cytokine storm, and promotion of phagocytosis.[57,58] To mimic the disease scenario in vivo, we used in vitro transcribed SARS-CoV-2 RNA to transfect HMC3 cells and induce their activation for subsequent pro-inflammatory responses.

Initially, we detected the expression of the spike protein in SARS-CoV-2 RNA-transfected HMC3 cells using immuno-fluorescent labelling with the RBD antibody (Figure 8b & c). Additionally, real-time Q-PCR studies confirmed the upregulation of pro-inflammatory responses in HMC3 cells upon exposure to SARS-CoV-2 by quantifying the gene expression of IL-1β and TNF-α (Figure 8d). Specifically, SARS-

https://doi.org/10.26434/chemrxiv-2023-vk4f4 **ORCID:** https://orcid.org/0000-0002-6484-9017 Content not peer-reviewed by ChemRxiv. **License:** CC BY-NC-ND 4.0

CoV-2-treated HMC3 cells exhibited a very intense fluorescence intensity of **PDM-NO** localized to lysosomes (Figure 8e). This was further confirmed by its well co-localization with the LysoT probe, as evidenced by the Pearson's coefficient (r) value of 0.91. The **PDM-NO**, being highly specific to the lysosome, displayed a turn-on response to the iNOS-induced lysosomal NO in SARS-CoV-2- RNA-transfected activated HMC3 cells. These findings indicate that SARS-CoV-2 RNA triggers pro-inflammatory responses in HMC3 cells, leading to lysosomal NO generation. The use of our lysosome-specific NO probe, **PDM-NO**, enables the visualization and detection of lysosomal NO response, providing valuable insights into the host cell-pathogen interactions during SARS-CoV-2 infection.

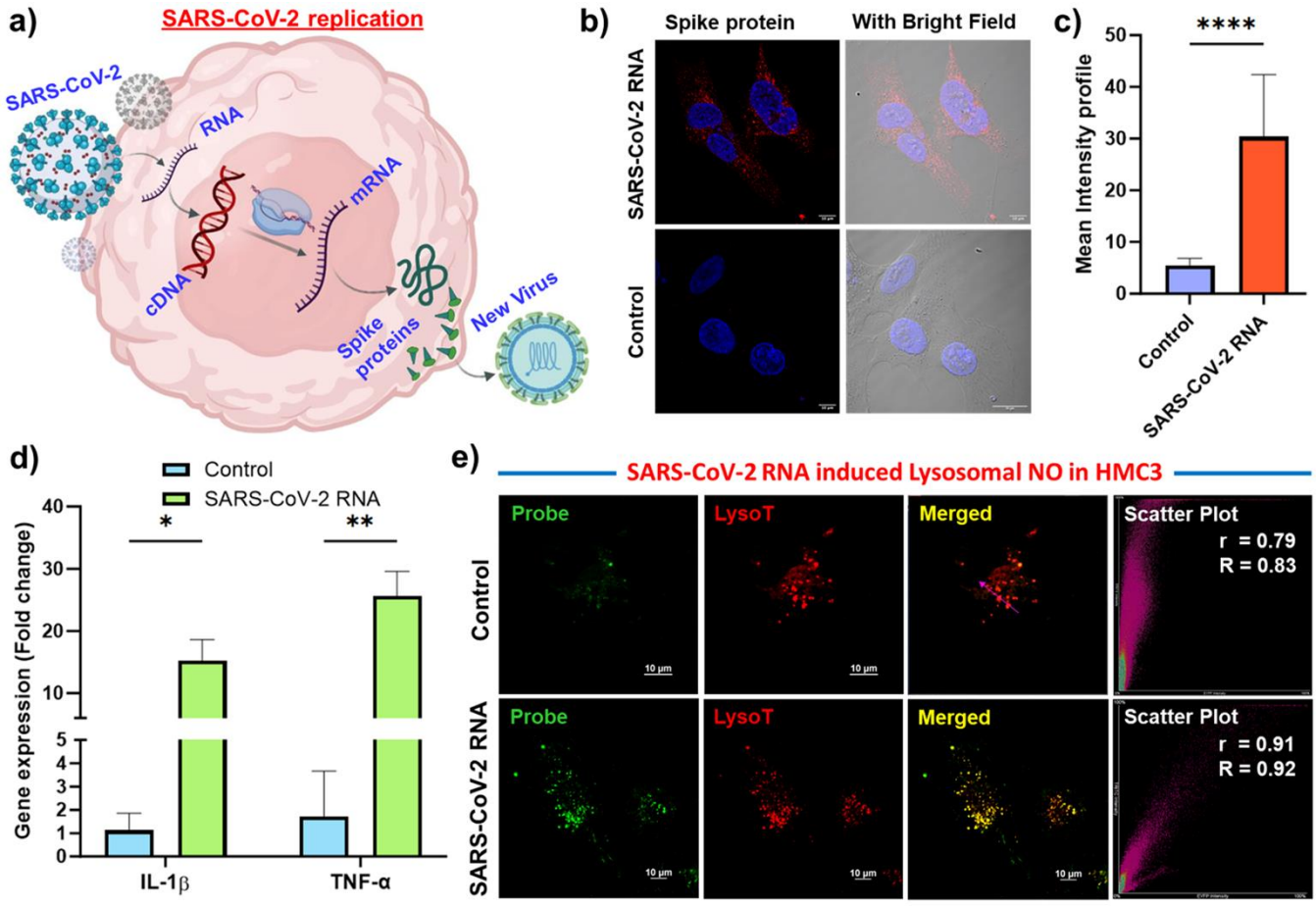

Figure 8. *a) Schematic representation of SARS-CoV-2 replication process. b) confocal microscopy imaging showing expression of spike protein in the cytoplasm of SARS-CoV-2 RNA transfected HMC3 cells compared to non-transfected control cells. c) The mean fluorescent intensity value of Figure 8b, was represented as a bar diagram. Data represent the means ± SEM (n = 3). * shows significance values compared to control, with a p-value <0.0001(unpaired t-test Welch's correction).* ***d)*** *Q-PCR validation of pro-inflammatory response of activated HMC3 through administration of SARS-CoV-2 RNA; Data represent the means ± SEM (n = 3). * shows significance values compared to control, * $p \leq 0.05$, ** $p \leq 0.01$. Statistical significance was calculated using Two-way ANOVA.* ***e)*** *Confocal fluorescence images for intracellular localization study of* ***PDM-NO*** *probe. Here, the HMC3 cells were administrated with a probe that was previously transfected with SARS-CoV-2 RNA. For labeling lysosomes, the cells were also treated with LysoTracker deep Red. Images were taken in the green channel (550−600 nm, ex. 488 nm)*

https://doi.org/10.26434/chemrxiv-2023-vk4f4 **ORCID:** https://orcid.org/0000-0002-6484-9017 Content not peer-reviewed by ChemRxiv. **License:** CC BY-NC-ND 4.0

*for **PDM-NO** and red channel (680−720 nm, ex. 640 nm) for LysoTracker deep Red and the corresponding scatter plots were represented. In the scatter plot, "r" and "R" represent Pearson's correlation coefficient and Mander's overlap coefficient, respectively. The image scale bar is 10 μm. Images were captured using a 60X oil emersion lens with 2X zoom.*

SARS-CoV-2 RNA-induced phagocytosis in HMC3. Currently, there is no effective way to study phagocytosis during SARS-CoV-2 invasion in any brain cellular model, including HMC3, due to the lack of a suitable tool. We have already observed an increase in lysosomal NO during the SARS-CoV-2 attack (Figure 8e). To address this limitation, we propose a method to study the phagocytosis process in HMC3 cells using confocal fluorescence imaging with our developed probe. Herein, **PDM-NO** (probe), LysoTracker red (LysoT), and *E. coli. P* were administrated with HMC3 cells, which was previously transfected with SARS-CoV-2 RNA for 24 hrs. As shown in Figure 9, we obtained perfectly overlapping images of the **PDM-NO** with LysoT and *E. Coli P*. Moreover, zoom images (marked a, b, c and d respectively of Figure 9) further confirmed the phagolysosomal fusion of bio-particles. In conclusion, our findings provide valuable insights into the phagocytosis process during SARS-CoV-2 invasion in HMC3 cells. This novel approach can potentially serve as a valuable tool for future studies investigating the mechanisms of viral invasion in brain cellular models. Most importantly, the probe can be implicated for screening the efficacy of any vaccine or therapeutics against SARS-CoV-2 that might be governed by NO dynamics to neutralize foreign pathogens through lysosomal degradation, i.e., phagocytosis.

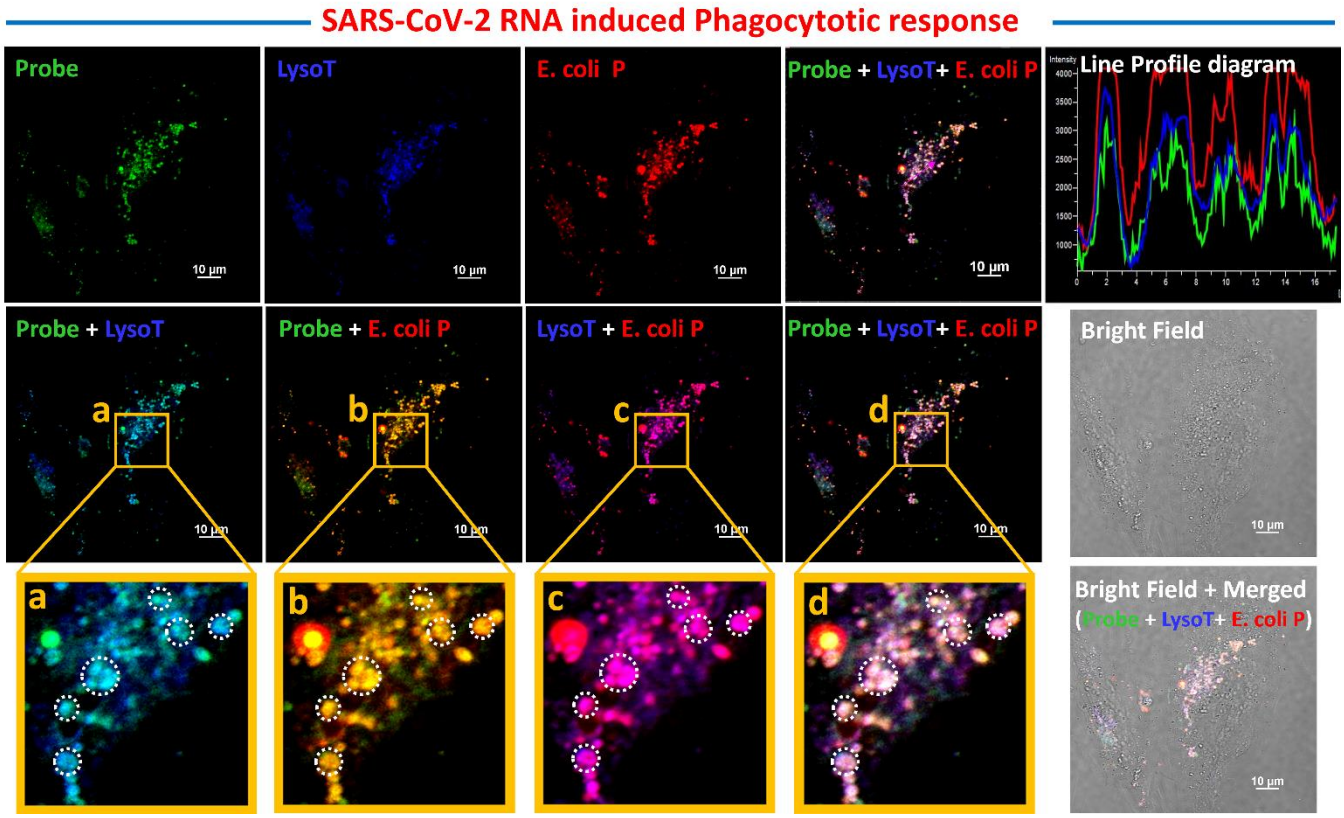

Figure 9. *Confocal fluorescence images for SARS-CoV-2 RNA-induced phagocytosis response study in HMC3 by **PDM-NO** probe. Here, the HMC3 cells were administrated with the probe, that was previously transfected with SARS-CoV-2 RNA for 24 hrs. For labeling lysosomes, the cells were also treated with LysoTracker deep Red. Images were taken in the green channel (550−600 nm, ex. 488 nm) for **PDM-NO**,*

https://doi.org/10.26434/chemrxiv-2023-vk4f4 **ORCID:** https://orcid.org/0000-0002-6484-9017 Content not peer-reviewed by ChemRxiv. **License:** CC BY-NC-ND 4.0

pseudo blue channel for LysoTracker deep red (680−720 nm, ex. 640 nm), and red channel (620−650 nm, ex. 560 nm) for E. coli. P. The line profile diagrams of the merged images are shown by arrow marks. The image scale bar is 10 μm. Images were captured using a 60X oil emersion lens with 2X zoom. The zoom images marked a, b, c and d represent the perfect merged images of the probe with LysoTracker, the probe with E. coli. P, LysoTracker with E. coli. P and the probe with LysoT+E. Coli. P respectively.

CONCLUSIONS

We have developed a unique synthetic strategy to create an OPD-derivative that exhibits an efficient fluorescent probe, named **PDM-NO**. It specifically targets lysosomes and allows for the detection of NO. This probe was designed by avoiding the tricky controlled amination reaction to render OPD derivative. It contains a positively charged pyridinium moiety with two morpholine units, which grants it excellent water solubility and lysosomal specificity. The probe demonstrates rapid responses to NO, with high sensitivity. The optical properties of **PDM-NO** are mostly regulated by PET which is well explained by DFT/TD-DFT/PCM theoretical calculations. The probe responds to NO by inhibiting the PET process, while the protonation of the morpholine unit interrupts the PET/EE process within the lysosomal pH window (pH 4.0 to 5.7). This unique probe shows significant potential for detecting lysosomal NO during inflammation in activated HMC3 cells. Furthermore, it also effectively monitors the phagocytosis process in activated microglia cells. The study highlights the importance of lysosomal nitric oxide in phagocytosis and provides valuable insights into the mechanisms of immune responses. **PDM-NO** enables the visualization and detection of lysosomal NO triggered by SARS-CoV-2 RNA. It offers valuable insights into the host cell-pathogen interactions during SARS-CoV-2 infection and phagocytosis process in HMC3 cells. This approach can potentially serve as a valuable tool for future studies, investigating the mechanisms of viral invasion in brain cellular models. Most importantly screening the efficacy of any vaccine or therapeutics against SARS-CoV-2 can also be studied.

ASSOCIATED CONTENT

Supporting Information. Supporting information containing details of the Materials and Methods; synthesis schemes; experimental procedures; results and discussion; supplementary quantum chemical data; cellular studies; characterization of the molecules; catalog of Cartesian coordinates; and references.

Conflicts of interest

The Shiv Nadar Institution of Eminence (SNIoE) has filed an invention disclosure form to protect part of the technology described in the study.

AUTHOR INFORMATION

Corresponding Author

*Dr. Animesh Samanta,

Molecular Sensors and Therapeutics (MST) Research Laboratory, Department of Chemistry, School of Natural Sciences, Shiv Nadar Institution of Eminence, Delhi NCR, NH 91, Tehsil Dadri, Uttar Pradesh, India 201314. E-mail: animesh.samanta@snu.edu.in

https://doi.org/10.26434/chemrxiv-2023-vk4f4 **ORCID:** https://orcid.org/0000-0002-6484-9017 Content not peer-reviewed by ChemRxiv. **License:** CC BY-NC-ND 4.0

*Dr. Soumya Pati,
Neurobiology and Disease Modeling Laboratory, Department of Life Sciences, School of Natural Sciences, Shiv Nadar Institution of Eminence, Delhi NCR, NH 91, Tehsil Dadri, Greater Noida, Uttar Pradesh, India 201314. E-mail: soumya.pati@snu.edu.in

*Dr. Shailja Singh,
Special Centre for Molecular Medicine, Jawaharlal Nehru University, New Delhi 110067, India. E-mail: shailjasingh@mail.jnu.ac.in

Funding Sources

A.S. is grateful to the DST-SERB, India, for the DST-Core Research Grant (CRG/2021/002313) and to the Shiv Nadar Foundation for funding. S.P. is grateful to the Shiv Nadar Foundation.

ACKNOWLEDGMENT

Ph.D. students S.M., A.M. are grateful to Shiv Nadar Institution of Eminence, Delhi NCR, and the Shiv Nadar Foundation for their research fellowships. We also acknowledge Prof. Milan Surjit for providing a pSFV2 vector containing the gene for the SARS-CoV-2 spike protein. The authors acknowledge the SNIoE DST-FIST grant [SR/FST/LS-1/2017/59(c)] for the confocal microscopy facility at Shiv Nadar Institution of Eminence, Delhi NCR. The authors are thankful to the High-Performance Cluster Computing (HPC) facility (MAGUS) of Shiv Nadar Institution of Eminence and other softwares including Scifinder, Chemdraw, origin etc.

REFERENCES

(1) Prinz, M.; Masuda, T.; Wheeler, M. A.; Quintana, F. J. Microglia and Central Nervous System-Associated Macrophages-From Origin to Disease Modulation. *Annu. Rev. Immunol.* **2021**, *39*, 251–277. https://doi.org/10.1146/annurev-immunol-093019-110159.

(2) Bachiller, S.; Jiménez-Ferrer, I.; Paulus, A.; Yang, Y.; Swanberg, M.; Deierborg, T.; Boza-Serrano, A. Microglia in Neurological Diseases: A Road Map to Brain-Disease Dependent-Inflammatory Response. *Front. Cell. Neurosci.* **2018**, *12* (December), 1–17. https://doi.org/10.3389/fncel.2018.00488.

(3) Colonna, M.; Butovsky, O. Microglia Function in the Central Nervous System During Health and Neurodegeneration. **2017**.

(4) Kwon, H. S.; Koh, S.-H. Neuroinflammation in Neurodegenerative Disorders: The Roles of Microglia and Astrocytes. *Transl. Neurodegener.* **2020**, *9* (1), 42. https://doi.org/10.1186/s40035-020-00221-2.

(5) Liu, Y.; Ho, R. C.-M.; Mak, A. Interleukin (IL)-6, Tumour Necrosis Factor Alpha (TNF-α) and Soluble Interleukin-2 Receptors (SIL-2R) Are Elevated in Patients with Major Depressive Disorder: A Meta-Analysis and Meta-Regression. *J. Affect. Disord.* **2012**, *139* (3), 230–239. https://doi.org/10.1016/j.jad.2011.08.003.

(6) Brás, J. P.; Bravo, J.; Freitas, J.; Barbosa, M. A.; Santos, S. G.; Summavielle, T.; Almeida, M. I. TNF-Alpha-Induced Microglia Activation Requires MiR-342: Impact on NF-KB Signaling and Neurotoxicity. *Cell Death Dis.* **2020**, *11* (6), 415. https://doi.org/10.1038/s41419-020-2626-6.

(7) Cai, Y.; Liu, J.; Wang, B.; Sun, M.; Yang, H. Microglia in the Neuroinflammatory Pathogenesis of

https://doi.org/10.26434/chemrxiv-2023-vk4f4 **ORCID:** https://orcid.org/0000-0002-6484-9017 Content not peer-reviewed by ChemRxiv. **License:** CC BY-NC-ND 4.0

Alzheimer's Disease and Related Therapeutic Targets. *Front. Immunol.* **2022**, *13*, 856376. https://doi.org/10.3389/fimmu.2022.856376.

(8) Wang, W.-Y.; Tan, M.-S.; Yu, J.-T.; Tan, L. Role of Pro-Inflammatory Cytokines Released from Microglia in Alzheimer's Disease. *Ann. Transl. Med.* **2015**, *3* (10), 136. https://doi.org/10.3978/j.issn.2305-5839.2015.03.49.

(9) Janda, E.; Boi, L.; Carta, A. R. Microglial Phagocytosis and Its Regulation: A Therapeutic Target in Parkinson's Disease? *Front. Mol. Neurosci.* **2018**, *11* (April), 1–8. https://doi.org/10.3389/fnmol.2018.00144.

(10) Fu, R.; Shen, Q.; Xu, P.; Luo, J. J.; Tang, Y. Phagocytosis of Microglia in the Central Nervous System Diseases. *Mol. Neurobiol.* **2014**, *49* (3), 1422–1434. https://doi.org/10.1007/s12035-013-8620-6.

(11) Galloway, D. A.; Phillips, A. E. M.; Owen, D. R. J.; Moore, C. S. Phagocytosis in the Brain: Homeostasis and Disease. *Front. Immunol.* **2019**, *10*, 790. https://doi.org/10.3389/fimmu.2019.00790.

(12) Chen, W.; Zhang, Y.; Zhai, X.; Xie, L.; Guo, Y.; Chen, C.; Li, Y.; Wang, F.; Zhu, Z.; Zheng, L.; Wan, J.; Li, P. Microglial Phagocytosis and Regulatory Mechanisms after Stroke. *J. Cereb. Blood Flow Metab.* **2022**, *42* (9), 1579–1596. https://doi.org/10.1177/0271678X221098841.

(13) Sarkar, S.; Korolchuk, V. I.; Renna, M.; Imarisio, S.; Fleming, A.; Williams, A.; Garcia-Arencibia, M.; Rose, C.; Luo, S.; Underwood, B. R.; Kroemer, G.; O'Kane, C. J.; Rubinsztein, D. C. Complex Inhibitory Effects of Nitric Oxide on Autophagy. *Mol. Cell* **2011**, *43* (1), 19–32. https://doi.org/10.1016/j.molcel.2011.04.029.

(14) Janabi, N.; Chabrier, S.; Tardieu, M. Endogenous Nitric Oxide Activates Prostaglandin F2 Alpha Production in Human Microglial Cells but Not in Astrocytes: A Study of Interactions between Eicosanoids, Nitric Oxide, and Superoxide Anion (O2-) Regulatory Pathways. *J. Immunol.* **1996**, *157* (5), 2129–2135.

(15) Ding, M.; St Pierre, B. A.; Parkinson, J. F.; Medberry, P.; Wong, J. L.; Rogers, N. E.; Ignarro, L. J.; Merrill, J. E. Inducible Nitric-Oxide Synthase and Nitric Oxide Production in Human Fetal Astrocytes and Microglia. A Kinetic Analysis. *J. Biol. Chem.* **1997**, *272* (17), 11327–11335. https://doi.org/10.1074/jbc.272.17.11327.

(16) Xiao, R.; Li, S.; Cao, Q.; Wang, X.; Yan, Q.; Tu, X.; Zhu, Y.; Zhu, F. Human Endogenous Retrovirus W Env Increases Nitric Oxide Production and Enhances the Migration Ability of Microglia by Regulating the Expression of Inducible Nitric Oxide Synthase. *Virol. Sin.* **2017**, *32* (3), 216–225. https://doi.org/10.1007/s12250-017-3997-4.

(17) Combs, C. K.; Colleen Karlo, J.; Kao, S. C.; Landreth, G. E. β-Amyloid Stimulation of Microglia Anti Monocytes Results in TNFα-Dependent Expression of Inducible Nitric Oxide Synthase and Neuronal Apoptosis. *J. Neurosci.* **2001**, *21* (4), 1179–1188. https://doi.org/10.1523/jneurosci.21-04-01179.2001.

(18) Muzio, L.; Viotti, A.; Martino, G. Microglia in Neuroinflammation and Neurodegeneration: From Understanding to Therapy. *Front. Neurosci.* **2021**, *15*, 742065. https://doi.org/10.3389/fnins.2021.742065.

(19) Lull, M. E.; Block, M. L. Microglial Activation and Chronic Neurodegeneration. *Neurother. J. Am. Soc. Exp. Neurother.* **2010**, *7* (4), 354–365. https://doi.org/10.1016/j.nurt.2010.05.014.

(20) Scheiblich, H.; Bicker, G. Nitric Oxide Regulates Antagonistically Phagocytic and Neurite Outgrowth Inhibiting Capacities of Microglia. *Dev. Neurobiol.* **2016**, *76* (5), 566–584.

https://doi.org/10.26434/chemrxiv-2023-vk4f4 **ORCID:** https://orcid.org/0000-0002-6484-9017 Content not peer-reviewed by ChemRxiv. **License:** CC BY-NC-ND 4.0

https://doi.org/10.1002/dneu.22333.

(21) Zhang, W.; Xiao, D.; Mao, Q.; Xia, H. Role of Neuroinflammation in Neurodegeneration Development. *Signal Transduct. Target. Ther.* **2023**, *8* (1), 267. https://doi.org/10.1038/s41392-023-01486-5.

(22) Dello Russo, C.; Cappoli, N.; Coletta, I.; Mezzogori, D.; Paciello, F.; Pozzoli, G.; Navarra, P.; Battaglia, A. The Human Microglial HMC3 Cell Line: Where Do We Stand? A Systematic Literature Review. *J. Neuroinflammation* **2018**, *15* (1), 1–24. https://doi.org/10.1186/s12974-018-1288-0.

(23) Navis, A. A Review of Neurological Symptoms in Long COVID and Clinical Management. *Semin. Neurol.* **2023**, *43* (2), 286–296. https://doi.org/10.1055/s-0043-1767781.

(24) Klein, R.; Soung, A.; Sissoko, C.; Nordvig, A.; Canoll, P.; Mariani, M.; Jiang, X.; Bricker, T.; Goldman, J.; Rosoklija, G.; Arango, V.; Underwood, M.; Mann, J. J.; Boon, A.; Dowrk, A.; Boldrini, M. COVID-19 Induces Neuroinflammation and Loss of Hippocampal Neurogenesis. *Research square*. United States October 2021. https://doi.org/10.21203/rs.3.rs-1031824/v1.

(25) Braga, J.; Lepra, M.; Kish, S. J.; Rusjan, P. M.; Nasser, Z.; Verhoeff, N.; Vasdev, N.; Bagby, M.; Boileau, I.; Husain, M. I.; Kolla, N.; Garcia, A.; Chao, T.; Mizrahi, R.; Faiz, K.; Vieira, E. L.; Meyer, J. H. Neuroinflammation After COVID-19 With Persistent Depressive and Cognitive Symptoms. *JAMA psychiatry* **2023**, *80* (8), 787–795. https://doi.org/10.1001/jamapsychiatry.2023.1321.

(26) Almutairi, M. M.; Sivandzade, F.; Albekairi, T. H.; Alqahtani, F.; Cucullo, L. Neuroinflammation and Its Impact on the Pathogenesis of COVID-19. *Front. Med.* **2021**, *8* (November), 1–14. https://doi.org/10.3389/fmed.2021.745789.

(27) Franke, C.; Berlit, P.; Prüss, H. Neurological Manifestations of Post-COVID-19 Syndrome S1-Guideline of the German Society of Neurology. *Neurol. Res. Pract.* **2022**, *4* (1), 28. https://doi.org/10.1186/s42466-022-00191-y.

(28) Hegna, E.; Rački, V.; Hero, M.; Papić, E.; Rožmarić, G.; Radović, K.; Komen, V.; Bralić, M.; Škifić, M. L.; Bonifačić, D.; Tomić, Z.; Perković, O.; Vuletić, V. Post-COVID-19 Syndrome in Neurology Patients: A Single Center Experience. *Pathog. (Basel, Switzerland)* **2023**, *12* (6). https://doi.org/10.3390/pathogens12060796.

(29) Mingoti, M. E. D.; Bertollo, A. G.; Simões, J. L. B.; Francisco, G. R.; Bagatini, M. D.; Ignácio, Z. M. COVID-19, Oxidative Stress, and Neuroinflammation in the Depression Route. *J. Mol. Neurosci.* **2022**, *72* (6), 1166–1181. https://doi.org/10.1007/s12031-022-02004-y.

(30) Leszek, J.; Barreto, G. E.; Gąsiorowski, K.; Koutsouraki, E.; Ávila-Rodrigues, M.; Aliev, G. Inflammatory Mechanisms and Oxidative Stress as Key Factors Responsible for Progression of Neurodegeneration: Role of Brain Innate Immune System. *CNS Neurol. Disord. Drug Targets* **2016**, *15* (3), 329–336. https://doi.org/10.2174/1871527315666160202125914.

(31) Mosley, R. L.; Benner, E. J.; Kadiu, I.; Thomas, M.; Boska, M. D.; Hasan, K.; Laurie, C.; Gendelman, H. E. Neuroinflammation, Oxidative Stress and the Pathogenesis of Parkinson's Disease. *Clin. Neurosci. Res.* **2006**, *6* (5), 261–281. https://doi.org/10.1016/j.cnr.2006.09.006.

(32) Vollbracht, C.; Kraft, K. Oxidative Stress and Hyper-Inflammation as Major Drivers of Severe COVID-19 and Long COVID: Implications for the Benefit of High-Dose Intravenous Vitamin C. *Front. Pharmacol.* **2022**, *13*, 899198. https://doi.org/10.3389/fphar.2022.899198.

(33) Käufer, C.; Schreiber, C. S.; Hartke, A.-S.; Denden, I.; Stanelle-Bertram, S.; Beck, S.; Kouassi, N. M.; Beythien, G.; Becker, K.; Schreiner, T.; Schaumburg, B.; Beineke, A.; Baumgärtner, W.;

https://doi.org/10.26434/chemrxiv-2023-vk4f4 **ORCID:** https://orcid.org/0000-0002-6484-9017 Content not peer-reviewed by ChemRxiv. **License:** CC BY-NC-ND 4.0

Gabriel, G.; Richter, F. Microgliosis and Neuronal Proteinopathy in Brain Persist beyond Viral Clearance in SARS-CoV-2 Hamster Model. *EBioMedicine* **2022**, *79*, 103999. https://doi.org/10.1016/j.ebiom.2022.103999.

(34) Jeong, G. U.; Lyu, J.; Kim, K.-D.; Chung, Y. C.; Yoon, G. Y.; Lee, S.; Hwang, I.; Shin, W.-H.; Ko, J.; Lee, J.-Y.; Kwon, Y.-C. SARS-CoV-2 Infection of Microglia Elicits Proinflammatory Activation and Apoptotic Cell Death. *Microbiol. Spectr.* **2022**, *10* (3), e0109122. https://doi.org/10.1128/spectrum.01091-22.

(35) Wallach, T.; Raden, M.; Hinkelmann, L.; Brehm, M.; Rabsch, D.; Weidling, H.; Krüger, C.; Kettenmann, H.; Backofen, R.; Lehnardt, S. Distinct SARS-CoV-2 RNA Fragments Activate Toll-like Receptors 7 and 8 and Induce Cytokine Release from Human Macrophages and Microglia. *Front. Immunol.* **2022**, *13*, 1066456. https://doi.org/10.3389/fimmu.2022.1066456.

(36) Salvi, V.; Nguyen, H. O.; Sozio, F.; Schioppa, T.; Gaudenzi, C.; Laffranchi, M.; Scapini, P.; Passari, M.; Barbazza, I.; Tiberio, L.; Tamassia, N.; Garlanda, C.; Del Prete, A.; Cassatella, M. A.; Mantovani, A.; Sozzani, S.; Bosisio, D. SARS-CoV-2-Associated SsRNAs Activate Inflammation and Immunity via TLR7/8. *JCI insight* **2021**, *6* (18). https://doi.org/10.1172/jci.insight.150542.

(37) Huo, Y.; Miao, J.; Fang, J.; Shi, H.; Wang, J.; Guo, W. Aromatic Secondary Amine-Functionalized Fluorescent NO Probes: Improved Detection Sensitivity for NO and Potential Applications in Cancer Immunotherapy Studies. *Chem. Sci.* **2019**, *10* (1), 145–152. https://doi.org/10.1039/C8SC03694B.

(38) Li, H.; Wan, A. Fluorescent Probes for Real-Time Measurement of Nitric Oxide in Living Cells. *Analyst* **2015**, *140* (21), 7129–7141. https://doi.org/10.1039/c5an01628b.

(39) Wang, L.; Zhang, J.; An, X.; Duan, H. Recent Progress on the Organic and Metal Complex-Based Fluorescent Probes for Monitoring Nitric Oxide in Living Biological Systems. *Org. Biomol. Chem.* **2020**, *18* (8), 1522–1549. https://doi.org/10.1039/c9ob02561h.

(40) Hou, J. T.; Yu, K. K.; Sunwoo, K.; Kim, W. Y.; Koo, S.; Wang, J.; Ren, W. X.; Wang, S.; Yu, X. Q.; Kim, J. S. Fluorescent Imaging of Reactive Oxygen and Nitrogen Species Associated with Pathophysiological Processes. *Chem* **2020**, *6* (4), 832–866. https://doi.org/10.1016/j.chempr.2019.12.005.

(41) Sasaki, E.; Kojima, H.; Nishimatsu, H.; Urano, Y.; Kikuchi, K.; Hirata, Y.; Nagano, T. Highly Sensitive Near-Infrared Fluorescent Probes for Nitric Oxide and Their Application to Isolated Organs. *J. Am. Chem. Soc.* **2005**, *127* (11), 3684–3685. https://doi.org/10.1021/ja042967z.

(42) Nakai, Y.; Yamamoto. NII-Electronic Library Service. *Chem. Pharm. Bull.* **1984**, *32* (2), 685–691.

(43) Chen, X.-X.; Niu, L.-Y.; Shao, N.; Yang, Q.-Z. BODIPY-Based Fluorescent Probe for Dual-Channel Detection of Nitric Oxide and Glutathione: Visualization of Cross-Talk in Living Cells. *Anal. Chem.* **2019**, *91* (7), 4301–4306. https://doi.org/10.1021/acs.analchem.9b00169.

(44) Kojima, H.; Hirotani, M.; Urano, Y.; Kikuchi, K.; Higuchi, T.; Nagano, T. Fluorescent Indicators for Nitric Oxide Based on Rhodamine Chromophore. *Tetrahedron Lett.* **2000**, *41* (1), 69–72. https://doi.org/10.1016/S0040-4039(99)02002-X.

(45) Kojima, H.; Nakatsubo, N.; Kikuchi, K.; Kawahara, S.; Kirino, Y.; Nagoshi, H.; Hirata, Y.; Nagano, T. Detection and Imaging of Nitric Oxide with Novel Fluorescent Indicators: Diaminofluoresceins. *Anal. Chem.* **1998**, *70* (13), 2446–2453. https://doi.org/10.1021/ac9801723.

(46) Gabe, Y.; Urano, Y.; Kikuchi, K.; Kojima, H.; Nagano, T. Highly Sensitive Fluorescence Probes for Nitric Oxide Based on Boron Dipyrromethene Chromophore - Rational Design of Potentially Useful Bioimaging Fluorescence Probe. *J. Am. Chem. Soc.* **2004**, *126* (10), 3357–3367.

https://doi.org/10.26434/chemrxiv-2023-vk4f4 **ORCID:** https://orcid.org/0000-0002-6484-9017 Content not peer-reviewed by ChemRxiv. **License:** CC BY-NC-ND 4.0

https://doi.org/10.1021/ja037944j.

(47) Goldman, S. D. B.; Funk, R. S.; Rajewski, R. A.; Krise, J. P. Mechanisms of Amine Accumulation in, and Egress from, Lysosomes. *Bioanalysis* **2009**, *1* (8), 1445–1459. https://doi.org/10.4155/bio.09.128.

(48) Munan, S.; Kottarathil, S.; Joseph, M. M.; Jana, A.; Ali, M.; Mapa, K.; Maiti, K. K.; Samanta, A. IndiFluors: A New Full-Visible Color-Tunable Donor–Acceptor–Donor (D1–A–D2) Fluorophore Family for Ratiometric PH Imaging during Mitophagy. *ACS Sensors* **2022**. https://doi.org/10.1021/acssensors.1c02381.

(49) Munan, S.; Ali, M.; Yadav, R.; Mapa, K.; Samanta, A. PET- and ICT-Based Ratiometric Probe: An Unusual Phenomenon of Morpholine-Conjugated Fluorophore for Mitochondrial PH Mapping during Mitophagy. *Anal. Chem.* **2022**, *94* (33), 11633–11642. https://doi.org/10.1021/acs.analchem.2c02177.

(50) Ishijima, T.; Nakajima, K. Inflammatory Cytokines TNFα, IL-1β, and IL-6 Are Induced in Endotoxin- Stimulated Microglia through Different Signaling Cascades. *Sci. Prog.* **2021**, *104* (4), 368504211054985. https://doi.org/10.1177/00368504211054985.

(51) Lively, S.; Schlichter, L. C. Microglia Responses to Pro-Inflammatory Stimuli (LPS, IFNγ+TNFα) and Reprogramming by Resolving Cytokines (IL-4, IL-10). *Front. Cell. Neurosci.* **2018**, *12* (July), 1–19. https://doi.org/10.3389/fncel.2018.00215.

(52) Fan, Y.; Xie, L.; Chung, C. Y. Signaling Pathways Controlling Microglia Chemotaxis. *Mol. Cells* **2017**, *40* (3), 163–168. https://doi.org/10.14348/molcells.2017.0011.

(53) Gray, M. A.; Choy, C. H.; Dayam, R. M.; Ospina-Escobar, E.; Somerville, A.; Xiao, X.; Ferguson, S. M.; Botelho, R. J. Phagocytosis Enhances Lysosomal and Bactericidal Properties by Activating the Transcription Factor TFEB. *Curr. Biol.* **2016**, *26* (15), 1955–1964. https://doi.org/10.1016/j.cub.2016.05.070.

(54) Hipolito, V. E. B.; Ospina-Escobar, E.; Botelho, R. J. Lysosome Remodelling and Adaptation during Phagocyte Activation. *Cell. Microbiol.* **2018**, *20* (4), e12824. https://doi.org/https://doi.org/10.1111/cmi.12824.

(55) V'kovski, P.; Kratzel, A.; Steiner, S.; Stalder, H.; Thiel, V. Coronavirus Biology and Replication: Implications for SARS-CoV-2. *Nat. Rev. Microbiol.* **2021**, *19* (3), 155–170. https://doi.org/10.1038/s41579-020-00468-6.

(56) Ghosh, S.; Dellibovi-Ragheb, T. A.; Kerviel, A.; Pak, E.; Qiu, Q.; Fisher, M.; Takvorian, P. M.; Bleck, C.; Hsu, V. W.; Fehr, A. R.; Perlman, S.; Achar, S. R.; Straus, M. R.; Whittaker, G. R.; de Haan, C. A. M.; Kehrl, J.; Altan-Bonnet, G.; Altan-Bonnet, N. β-Coronaviruses Use Lysosomes for Egress Instead of the Biosynthetic Secretory Pathway. *Cell* **2020**, *183* (6), 1520-1535.e14. https://doi.org/10.1016/j.cell.2020.10.039.

(57) Aboudounya, M. M.; Heads, R. J. COVID-19 and Toll-Like Receptor 4 (TLR4): SARS-CoV-2 May Bind and Activate TLR4 to Increase ACE2 Expression, Facilitating Entry and Causing Hyperinflammation. *Mediators Inflamm.* **2021**, *2021*, 8874339. https://doi.org/10.1155/2021/8874339.

(58) Khan, S.; Shafiei, M. S.; Longoria, C.; Schoggins, J. W.; Savani, R. C.; Zaki, H. SARS-CoV-2 Spike Protein Induces Inflammation via TLR2-Dependent Activation of the NF-KB Pathway. *Elife* **2021**, *10*, e68563. https://doi.org/10.7554/eLife.68563.

https://doi.org/10.26434/chemrxiv-2023-vk4f4 **ORCID:** https://orcid.org/0000-0002-6484-9017 Content not peer-reviewed by ChemRxiv. **License:** CC BY-NC-ND 4.0

"for TOC Only"

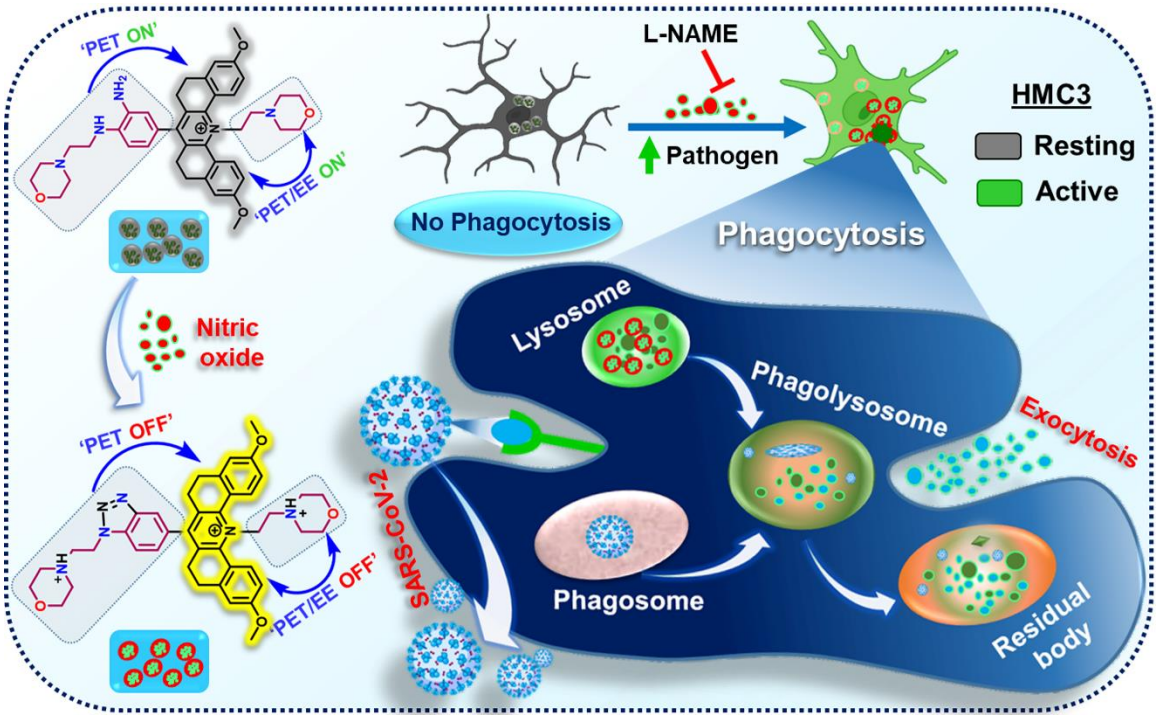

https://doi.org/10.26434/chemrxiv-2023-vk4f4 **ORCID:** https://orcid.org/0000-0002-6484-9017 Content not peer-reviewed by ChemRxiv. **License:** CC BY-NC-ND 4.0